



Development of spectral indices for detecting and identifying plant diseases

A.-K. Mahlein ^{a,*}, T. Rumpf ^{b,1}, P. Welke ^b, H.-W. Dehne ^a, L. Plümer ^b, U. Steiner ^a, E.-C. Oerke ^a

^a Institute of Crop Science and Resource Conservation (INRES-Phytomedicine), University of Bonn, Nussallee 9, D-53115 Bonn, Germany

^b Institute of Geodesy and Geoinformation, Department of Geoinformation, University of Bonn, Meckenheimer Allee 172, D-53115 Bonn, Germany

ARTICLE INFO

Article history:

Received 26 October 2011
Received in revised form 28 August 2012
Accepted 19 September 2012
Available online 24 October 2012

Keywords:

Spectral disease indices
Hyperspectral reflectance
Band selection
Sugar beet
Plant diseases
Precision crop protection
Cercospora leaf spot
Powdery mildew
Sugar beet rust

ABSTRACT

Spectral vegetation indices (SVIs) have been shown to be useful for an indirect detection of plant diseases. However, these indices have not been evaluated to detect or to differentiate between plant diseases on crop plants. The aim of this study was to develop specific spectral disease indices (SDIs) for the detection of diseases in crops. Sugar beet plants and the three leaf diseases *Cercospora* leaf spot, sugar beet rust and powdery mildew were used as model system. Hyperspectral signatures of healthy and diseased sugar beet leaves were assessed with a non-imaging spectroradiometer at different developing stages and disease severities of pathogens. Significant and most relevant wavelengths and two band normalized differences from 450 to 950 nm, describing the impact of a disease on sugar beet leaves were extracted from the data-set using the RELIEF-F algorithm. To develop hyperspectral indices for the detection of sugar beet diseases the best weighted combination of a single wavelength and a normalized wavelength difference was exhaustively searched testing all possible combinations. The optimized disease indices were tested for their ability to detect and to classify healthy and diseased sugar beet leaves. With a high accuracy and sensitivity healthy sugar beet leaves and leaves, infected with *Cercospora* leaf spot, sugar beet rust and powdery mildew were classified (balanced classification accuracy: 89%, 92%, 87%, 85%, respectively). Spectral disease indices were also successfully applied on hyperspectral imaging data and on non-imaging data from a sugar beet field. Specific disease indices will improve disease detection, identification and monitoring in precision agriculture applications.

© 2012 Elsevier Inc. All rights reserved.

1. Introduction

Near-range and remote sensing methods, like hyper- and multispectral sensors or thermography possess multiple opportunities to increase the productivity of agricultural production systems (Oerke et al., 2006; Steiner et al., 2008). Remote sensing technologies can provide an automatic and objective alternative to visual disease assessment of plant diseases (Hillnhütter & Mahlein, 2008; Mahlein et al., 2012a; Nutter et al., 1990). Many researchers have shown the capabilities of remote sensing techniques in the area of agriculture and crop production (i.e. Doraiswamy et al. (2003); Galvao et al. (2009); Thenkabail et al. (2000)) and also in the field of plant disease detection. Hillnhütter et al. (2011), Mahlein et al. (2010, 2012 b, a), Moshou et al. (2004) and Steddom et al. (2005) have proven the potential of spectral sensor systems for the detection of fungal diseases.

Efficient use of spectral reflectance measurements for disease detection relies on the identification of most significant spectral wavelength, highly correlated to a specific disease. Depending on the application area and aim, just a few regions of the spectrum are of interest. In the visible region from 400 to 700 nm, the composition of pigments has a predominant impact on the spectral signature (Blackburn & Steele, 1999;

Gitelson et al., 2002). The near infrared from 700 to 1100 nm is mainly influenced by structural leaf traits and water content (Jacquemoud & Baret, 1990).

The use of spectral vegetation indices (SVIs) is a common method to analyze and to detect changes in plant physiology and chemistry. These indices, based on the information of few wavelengths have been developed to specify different plant parameters, such as pigment content (Blackburn, 1998a; Gitelson et al., 2002; Peñuelas et al., 1995), leaf area (Rouse et al., 1974) or water content (Peñuelas et al., 1993). A quantitative relation between the trait of interest, i.e. high correlation to pigment or water content, and SVIs is typical. Several approaches however have shown that SVIs have additionally the potential to detect plant diseases (Hatfield et al., 2008; Thenkabail et al., 2000). But a quantitative statement or the identification of a specific disease based on common SVIs is not possible so far, since these indices lack disease specificity. Therefore, disease specific data analysis methods and algorithms are required. A combination of different wavelengths to so called spectral disease indices (SDI) can be useful to simplify disease detection by spectral sensors, since each disease influences the spectral signature in a characteristic way.

In contrast to common SVIs the developed SDIs aimed to detect diseased sugar beet leaves as well as to identify and differentiate one disease from others. Experiments under controlled conditions were performed to identify the most important spectral wavelength for plant disease detection and identification (Mahlein et al., 2010). A methodology for the

* Corresponding author. Tel.: +49 228 734 997.

E-mail address: amahlein@uni-bonn.de (A.-K. Mahlein).

¹ Both authors equally contributed to this work.

extraction and combination of most relevant wavelengths to SDIs was developed. For a reduction of data dimensionality each SDI consists of the combination of a single and a normalized wavelength difference according to Blackburn and Steele (1999), Carter and Miller (1994), Delalieux et al. (2009), and Thenkabail et al. (2000). To validate the transferability of the developed indices, independent data sets from field spectroscopy and from a hyperspectral camera were used.

Based on the above background, the main objective of this paper was (I) to identify disease specific single wavelengths and wavelength differences, (II) to combine these specific wavelengths to spectral disease indices, and (III) to approve the developed indices on independent datasets. Therefore a statistical approach was adopted to compute and to evaluate spectral disease indices.

2. Material and methods

2.1. Experimental setup

A data set of spectral signatures from healthy sugar beet leaves and from sugar beet leaves inoculated with foliar diseases was used as groundwork for DI development. A specific index was evaluated for each of the four classes (I) healthy, (II) *Cercospora* leaf spot, (III) powdery mildew and (IV) sugar beet rust. The spectral reflectance was assessed under constant conditions in a controlled environment, and experiments were repeated twice.

2.2. Plant cultivation and pathogen inoculation

Sugar beet plants, cultivar Paulette (KWS GmbH, Einbeck, Germany), were grown in a commercial substrate (Klasmann-Deilmann GmbH, Germany) in plastic pots (ϕ 13 cm) in a greenhouse at 23/20 °C (day/night), 60% relative humidity (RH) and a photo-period of 16 h ($>300 \mu\text{mol/m}^2 \text{ s}^{-1}$) per day. Plants were watered as necessary and fertilized weekly with 100 ml of a 0.2% solution of Poly Crescal (Aglukon GmbH, Düsseldorf, Germany).

For each class, 15 plants were inoculated with the pathogens when four leaves were fully developed. Production of inoculum of the pathogens *Cercospora beticola*, *Uromyces beta* and *Erysiphe betae* and inoculation of plants were carried out according to Mahlein et al. (2010). Each treatment consisted of 15 plants.

2.3. Measurement of leaf reflectance

Spectral reflectance was measured with a handheld non-imaging spectro-radiometer using a plant probe foreoptic with a leaf clip holder (ASD FieldSpec Pro FR spectrometer, Analytic Spectral Devices, Boulder, USA). The spectral range was from 350 nm to 1100 nm with a spectral resolution of 3 nm. Because the reflectance spectra data were noisy at the extremes, values between 400 nm and 1050 nm were analyzed. The contact probe foreoptic has a 10 mm field of view and an integrated 100 W halogen reflector lamp. The instrument was warmed up for 90 min previous to measurement to increase the quality and homogeneity of spectral data. Instrument optimization and reflectance calibration were performed prior to sample acquisition. The average of 25 dark-current measurements was calibrated to the average of 25 barium sulfate white reference (Spectralon, Labsphere, North Sutton, NH, USA) measurements. Because of the internal light source, the integration time was adjusted to 17 ms per scan constantly. Finally, reflectance spectra were obtained by determining the ratio of recorded sample data to data acquired for the white reflectance standard. Each sample scan represented an average of 25 reflectance spectra. Because reflectance spectra were assessed under constant light and temperature conditions with the plant probe foreoptic, pre-processing to smooth the spectrum and reduce signal noise was not necessary.

Data of infected and non-infected leaves were collected and recorded daily until 21 days after inoculation (dai). In each class, spectra from 15

plants and 2 leaves per plant from the adaxial leaf surface were taken. Disease severity caused by each pathogen was evaluated daily and classified according to Wolf and Verreet (2002). The experiment was repeated twice.

2.4. Development of specific disease indices

A statistical approach was adapted to compute and to evaluate SDIs. Fig. 1 summarizes the steps from spectral signatures to disease-specific

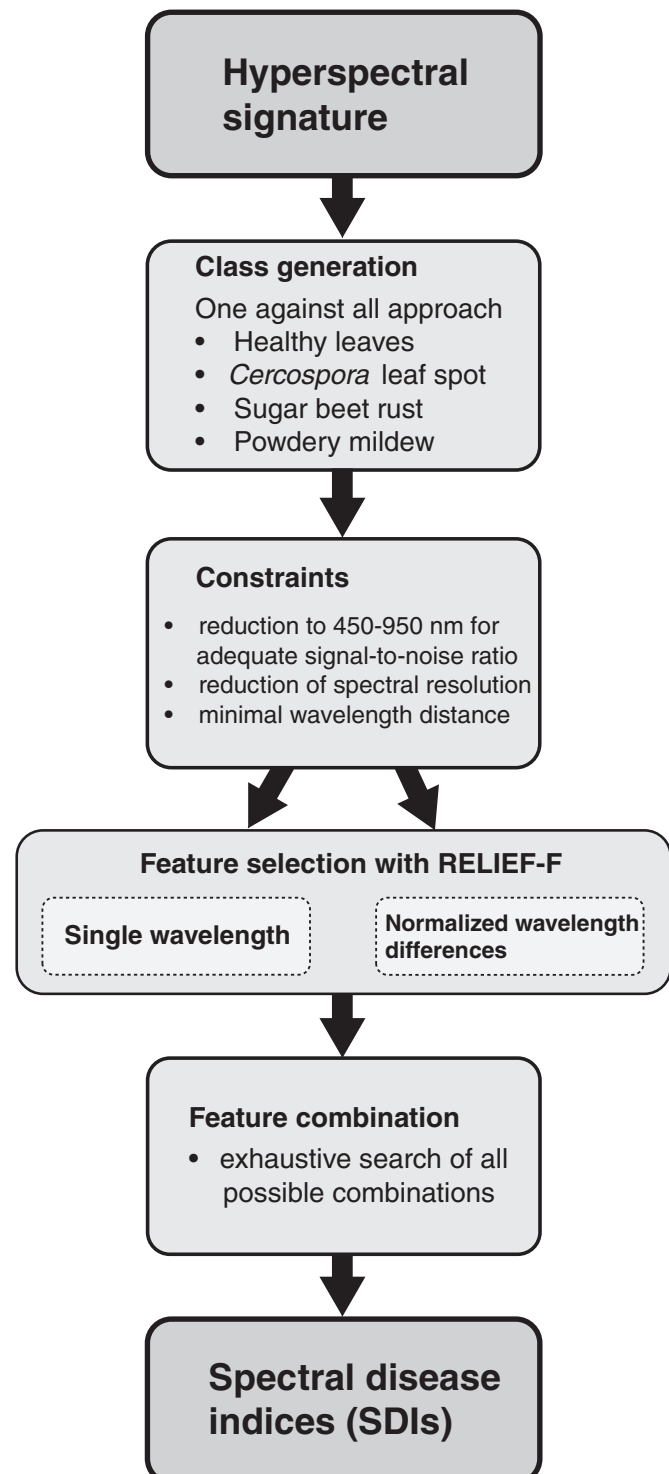


Fig. 1. Systematical approach and development of specific disease indices (DI) from hyperspectral reflectance data.

indices. Hyperspectral signature from the classes (I) healthy, (II) *Cercospora* leaf spot, (III) powdery mildew and (IV) sugar beet rust were the basis for the generation of SDIs.

Reflectance data from disease severities of 1 to 30% was used for index development to be sensitive to early disease stages and to use characteristic hyperspectral signatures of mature disease symptoms as a basis. Hyperspectral signatures of every class were compared to all other classes in order to ensure disease specificity in a one against all approach. Several constraints were set to reduce dimensionality of the data and to increase the robustness and transferability to other data sets in advance. Since wavelengths next to each other are highly correlated, the minimal distance between wavelengths combined in normalized differences was set to 50 nm (a counter plot indicating wavelength correlation can be found in the supplementary data, Appendix A). Further the spectral resolution was reduced to 6 nm due to high correlation between neighboring wavelengths. The developed indices aim at qualitatively recognizing a specific plant disease independent of disease severity. Thus a combination of a single wavelength and a normalized wavelength difference seemed suitable. A combination of two normalized two band wavelength differences was tested simultaneously and resulted in lower classification results. Single wavelengths are especially important to differentiate samples with higher disease severity. Differences were suitable to assess changes in the hyperspectral signature caused by *Cercospora* leaf spot and sugar beet rust, as the course of the disease cause opposed changes at different ranges on the hyperspectral signature. As powdery mildew, however, caused a parallel shift in the hyperspectral signature, normalized differences performed separation of powdery mildew and the other classes' best.

Before finding the best combination of single wavelength and wavelength difference, feature selection was necessary. The most relevant single wavelengths and wavelength differences were extracted by the RELIEF-F algorithm (Robnik-Šikonja & Kononenko, 2003) (for detailed information on feature selection and the RELIEF algorithm please see Appendix B in the supplementary data). The RELIEF algorithm (Kononenko, 1994) estimates the relevance of wavelength according to their goodness to separate samples of both classes which are near to each other. The advantage of the RELIEF-F algorithm is to correctly estimate the quality of features with strong dependencies. Moreover, the algorithm is robust against outliers. The RELIEF-F searches for the two nearest neighbors of a given sample. Each neighborhood consists of k samples. For a given k , 'hit' is the set of k nearest neighbors of the same class and 'miss' from the different class. In fact, the relevance of the wavelengths is determined by the sum of the Euclidean distance between nearest misses and nearest hits for all samples (List. 1).

Listing 1: Pseudo code of the Relief-F algorithm for two class classification

```

INPUT: A set of features  $F$ , a set of samples  $X$ ,
       a label function  $l$ , a number of iterations  $p \in \mathbb{N}$ 
       and a number of neighbors  $k \in \mathbb{N}$ 
OUTPUT: A set of feature weights  $w = \{w(F_1), \dots, w(F_m)\}$ 
Set  $w(F_i) := 0 \forall i \in \{0, \dots, m\}$ 
for  $i := 1$  to  $p$ 
  Pick  $x \in X$  at random
  Find  $k$  nearest hits  $A \subseteq X$  and nearest misses  $B \subseteq X$ 
  for  $j := 1$  to  $m$ 
     $w(F_j) := w(F_j) - \frac{1}{k} \sum_{a \in A} |x_j - a_j| + \frac{1}{k} \sum_{b \in B} |x_j - b_j|$ 
  end
end
Set  $w(F_i) := \frac{w(F_i)}{m} \forall i \in \{0, \dots, m\}$ 
return  $\{w(F_1), \dots, w(F_m)\}$ 
```

Finally, the best combination of an individual wavelength and a normalized wavelength difference has to be found. The best weighted 25% of single wavelengths and normalized wavelength differences

were included for SDI development. All possible combinations were exhaustively searched to find the best index with a related threshold for separating the index-specific class. Because of the high variance in hyperspectral signature between individual plants and high variance especially at low disease severities, the normalized wavelength difference is mandatory for building a specific index. Furthermore a weighting factor for the single wavelength has to be determined. We set the possible weights $-1, -0.5, 0, 0.5$ and 1 . The final indices were evaluated for their classification result using an 8-fold cross validation by stratified sampling. The balanced accuracy was used for classification accuracy, whereby both classes were equally weighted. The two independent data sets from two experiments afford optimal conditions to develop indices as robust as possible. In general all calculations were programmed in MATLAB 7.11 using parallel processing by an eight-core processor.

2.5. Comparison with common vegetation indices

The ability to identify disease with SDIs was tested and compared to vegetation indices from literature. The classification accuracies of the NDVI (Rouse et al., 1974), the PRI (Gamon et al., 1992), the ARI (Gitelson et al., 2001), the SIPI (Pefuelas et al., 1995), the mCAI (Laudien et al., 2003), the PSSRa, PSSRb, and PSSRc (Blackburn, 1998b), the GM1 and GM2 (Gitelson & Merzlyak, 1997), the ZM (Zarco-Tejada et al., 2001) and the TCARI/OSAVI (Haboudane et al., 2002) were compared to the developed SDIs using an 8-fold cross validation by stratified sampling.

2.6. Independent data sets

To test the transferability of the developed disease indices on independent data sets, non-imaging data from a field experiment and hyperspectral imaging data were used. The datasets were assessed with different sensors and under different measuring conditions.

2.6.1. Field data

A field experiment was conducted at the research station Klein-Altendorf ($50^{\circ}36'55.36''N, 7^{\circ}0'0.10''E$) of the University of Bonn in the growing season of 2008 as described by Mahlein et al. (2009). The field was divided in two treatments; treatment 1 without fungicide application in order to monitor the incidence of fungal diseases over the growing season; the plants of treatment 2 were treated once with the fungicide Spyrale® (Syngenta Agro GmbH; 1 l/ha, difenoconazol 100 g/l; fenpropidin 375 g/l) to avoid fungal infections. On September 9, 2008, spectral reflectance from sugar beet canopy was assessed using an ASD FieldSpecPro FR with a pistol grip foreoptic, which was placed 1 m above the sugar beet canopy constantly. The spectral range of the spectroradiometer was from 400 nm to 1050 nm. The spectral sampling interval was automatically interpolated from 1.4 nm to 1 nm steps using a linear equation by the ASD software. Instrument optimization and reflectance calibration were performed prior to sample acquisition. The average of 50 dark current measurements was calibrated to the average of 50 barium sulfate white reference (Spectralon, Labsphere, North Sutton, NH, USA) measurements. The integration time was adjusted to 34 ms per scan constantly. Finally reflectance spectra were obtained by determining the ratios of data acquired for a sample to data acquired for the white reflectance standard. Each sample scan represented an average of 50 reflectance spectra. Spectral reflectance and ground truth data, in particular incidence and severity of diseases were collected and geo-referenced at 50 sampling points.

2.6.2. Hyperspectral imaging data

Hyperspectral images from diseased sugar beet plants were taken using an imaging system. The hyperspectral imaging system combines an imaging spectrograph and a mirror scanner. The line scanning

spectrograph ImSpector V10E (Spectral Imaging Ltd., Oulu, Finland) has a spectral range from 400 to 1000 nm and a spectral resolution of up to 2.8 nm. The maximal image size of the 30 μm sensor slot results in 1600 pixels per line with a sensor pixel size of 0.0074 mm. Limited by the distance between target and sensor system (0.9 m) a spatial resolution of 0.29 mm per pixel was obtained. A mirror scanner (Spectral Imaging Ltd.) – maximal field of view 80° – mounted in front of the objective lens provided the second spatial dimension of images. The hyperspectral sensor system was mounted on a manual positioning XY-frame, surrounded by six ASD-Pro-Lamps (Analytical Spectral Devices Inc., Boulder, USA) radiating a near-solar light spectrum. The distance between lamps and leaves was 0.8 m with a vertical orientation of 45°. Imaging data were recorded in a dark chamber in order to realize optimal and reproducible illumination and constant measurement conditions. For subsequent calculation of reflectance, three images were grabbed. A dark current image was recorded by closing an internal shutter of the camera, followed by an image of a white reference bar (Spectral Imaging Ltd., Oulu, Finland), with the same horizontal size and on the same level as the object area, both with the same exposure time. Subsequently an image of the leaf area was recorded with improved exposure time. Calculation of reflectance, relative to a white reference bar and the dark current measurement were performed using the software ENVI 4.6 + IDL 7.0 (ITT Visual Information Solutions, Boulder, USA). Prior to the calculation of disease indices on imaging data the background was masked out. For detailed information on data assessment, data pre-processing and normalization see Mahlein et al. (2012b).

3. Results

3.1. Spectral signatures

First symptoms of *Cercospora* leaf spot appeared 6 dai, of powdery mildew 5 dai and sugar beet rust 8 dai, respectively. For the differentiation of leaf diseases based on reflectance measurement, spectral signatures at different disease severities have been measured and compared. Fig. 2A summarizes the averaged spectral signatures of healthy sugar beet leaves and sugar beet leaves with *Cercospora* leaf spot, powdery mildew, and sugar beet rust at disease severity of 10 to 30%, respectively. Compared to the spectra of healthy leaves, each disease gave a divergent, characteristic reflectance curve, strongly correlated to the occurrence of disease-specific symptoms. Reflectance of *C. beticola*-infected leaves increased in the VIS mostly in the green and red ranges of the spectrum between 500 and 700 nm and decreased from 700 to 900 nm. The slope at the red edge position between VIS and NIR decreased. A blue shift of the red edge position depending on *Cercospora* leaf spot disease severity was obvious. Reflectance of leaves colonized by the ectoparasite *E. betaee* rose consecutively within the measuring period and increased with disease severity (Fig. 2A). This increment was most distinctive in the VIS and less pronounced in the NIR. Powdery mildew rather affected the overall level of reflectance than the profile of spectra. Due to the small symptoms of the biotroph pathogen *U. betae* scattered on the leaf area, changes in reflectance spectra were comparatively low for sugar beet rust (Fig. 2A). Reflectance of leaves with 10 to 30% disease severity was high between 550 and 700 nm and low from 700 to 900 nm.

The variance of the dataset was analyzed by standard deviation of reflectance and by the absolute differences between the reflectance median (Fig. 2B). Standard deviation of diseased sugar beet leaves increased in the VIS from 400 to 700 nm and in the NIR from 720 to 780 nm with increasing disease severity. The reflectance difference likewise increased with disease severity. At a disease severity below 10% differences were detected in the VIS from 500 to 700 nm and around the red edge position. At disease severities in the range 10 to 30% increased obviously in the VIS with a peak around 700 nm. Reflectance differences at

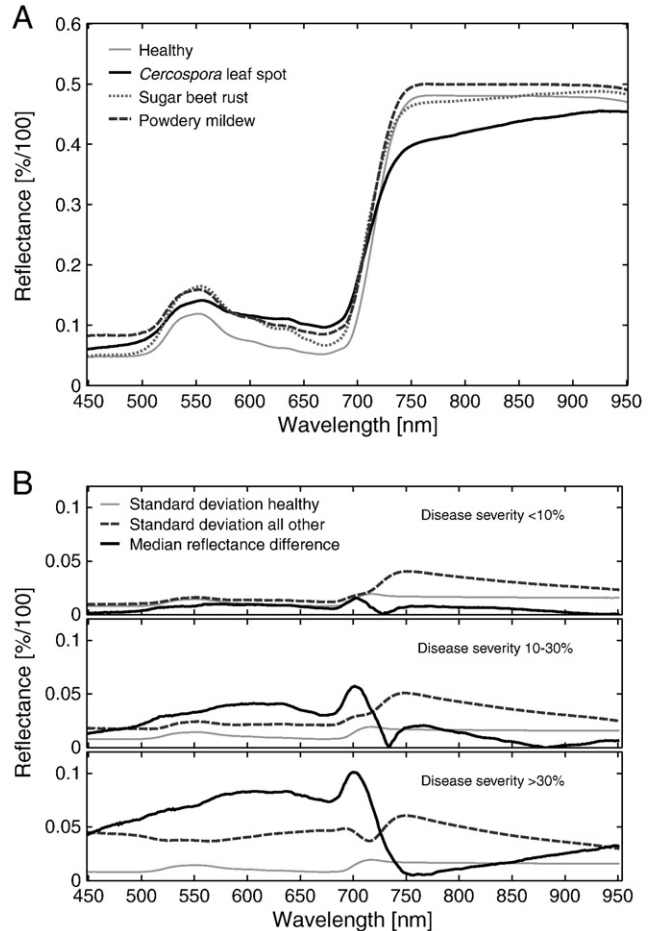


Fig. 2. Spectral signatures of healthy sugar beet leaves and sugar beet leaves with 10 to 30% disease severity of *Cercospora* leaf spot, sugar beet rust and powdery mildew, respectively; and differences between reflectance medians and standard deviation of healthy sugar beet leaves and diseased sugar beet leaves at different disease severities.

disease severities above >30% were high in the VIS and at the red edge position.

3.2. Spectral plant disease indices

For the evaluation of specific DIs the different classes were parted into two groups. In the first step a binary classification of healthy sugar beet leaves from diseased leaves was proven in a one against all approach. In addition to a binary classification of healthy and diseased sugar beet leaves, the detection and identification of plant diseases by specific SDIs were proven. Therefore disease specific indices, based on significant wavelengths were evaluated. To reduce the information of the entire spectrum, the most relevant single wavelengths and wavelength differences were evaluated. The result of this data reduction was the basis for index development.

Relevant single wavelengths for the classes were assessed calculating the RELIEF algorithm (Fig. 3). Single wavelengths of high relevance were from 670 to 690 nm (Fig. 3A). Single wavelengths around 500 nm, 690 nm and 730 nm were highly relevant for sugar beet leaves diseased with *Cercospora* leaf spot (Fig. 3C). Single wavelengths relevant to sugar beet rust infection according to the RELIEF-F algorithm were around 500 nm, 570 nm and 700 nm (Fig. 3E), and for powdery mildew infection at 450 and 720 nm (Fig. 3G).

The contour plot (Fig. 3B) visualizes normalized wavelength differences highly correlated to the class 'healthy'. High relevance was detected for normalized differences including reflectance difference between 600 and 670 nm and at 700 nm. Normalized reflectance

differences, highly correlated to *Cercospora* leaf spot included values around 550 nm and 700 nm (Fig. 3D), for sugar beet rust infected leaves from 500 to 600 nm and normalized wavelength differences including 700 nm (Fig. 3F), and for powdery mildew infection normalized wavelength differences between 500 and 600 nm (Fig. 3H).

Based on single wavelengths of high relevance according to the RELIEF algorithm and the two band normalized differences highly correlated to the class 'healthy', possible wavelength combinations and

algorithms for a class specific vegetation index were calculated. The final health-index (HI) is based on the absolute reflectance at 704 nm and the normalized reflectance difference 534 nm to 698 nm (Eq. (1)). Testing all possible wavelength combinations, the *Cercospora* leaf spot-index (CLSI) is based on the reflectance at 734 nm and the normalized reflectance difference of 698 nm and 570 nm (Eq. (2)). After this data dimensionality reduction the sugar beet rust-index (SBRI) was evaluated (Eq. (3)) based on reflectance at 704 nm and

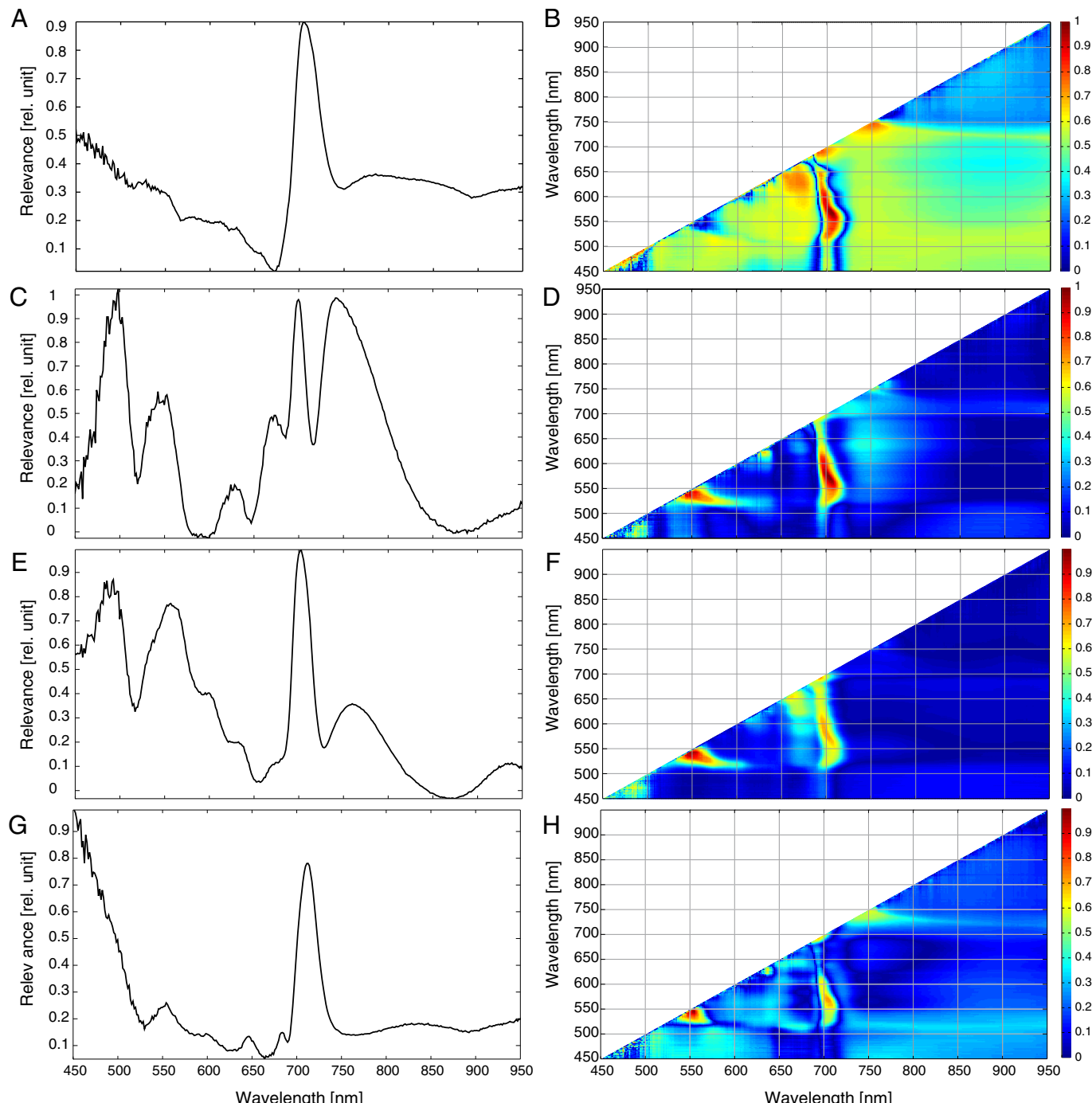


Fig. 3. Relevant single wavelengths for the class healthy sugar beet leaves (A), *Cercospora* leaf spot (C), sugar beet rust (E) and powdery mildew (G) diseased sugar beet leaves, according to the RELIEF-F algorithm, and contour plot for the relevance of all possible wavelength differences of the class label healthy (B), and the classes *Cercospora* leaf spot (D), sugar beet rust (F) and powdery mildew (H) at a disease severity of 10 to 30%, respectively. The color scale represents the level of relevance according to the RELIEF-F algorithm.

the normalized difference of 570 and 513 nm. Previous information resulted in the powdery mildew-index (PMI; Eq. (4)), related to absolute reflectance at 724 nm and the normalized reflectance difference of 520 nm and 584 nm.

$$\text{Healthy - index (HI)} : \frac{R534 - R698}{R534 + R698} - \frac{1}{2} \cdot R704 \quad (1)$$

$$\text{Cercospora leaf spot - index (CLSI)} : \frac{R698 - R570}{R698 + R570} - R734 \quad (2)$$

$$\text{Sugar beet rust - index (SBRI)} : \frac{R570 - R513}{R570 + R513} + \frac{1}{2} \cdot R704 \quad (3)$$

$$\text{Powdery mildew - index (PMI)} : \frac{R520 - R584}{R520 + R584} + R724 \quad (4)$$

The separation ability of the spectral disease indices is illustrated in Fig. 4, depending on the index value at different days after inoculation for each class. A threshold value was optimized to separate healthy from diseased sugar beet leaves. Classification based on the HI resulted in a classification accuracy of 89%, with a class precision of 93.5% for the classification of diseased sugar beet leaves and 85.5% for healthy sugar beet leaves (Table 1). The classification error for healthy sugar beet leaves was 5.2%, independently of disease severity. The classification error for diseased sugar beet leaves decreased with increasing disease

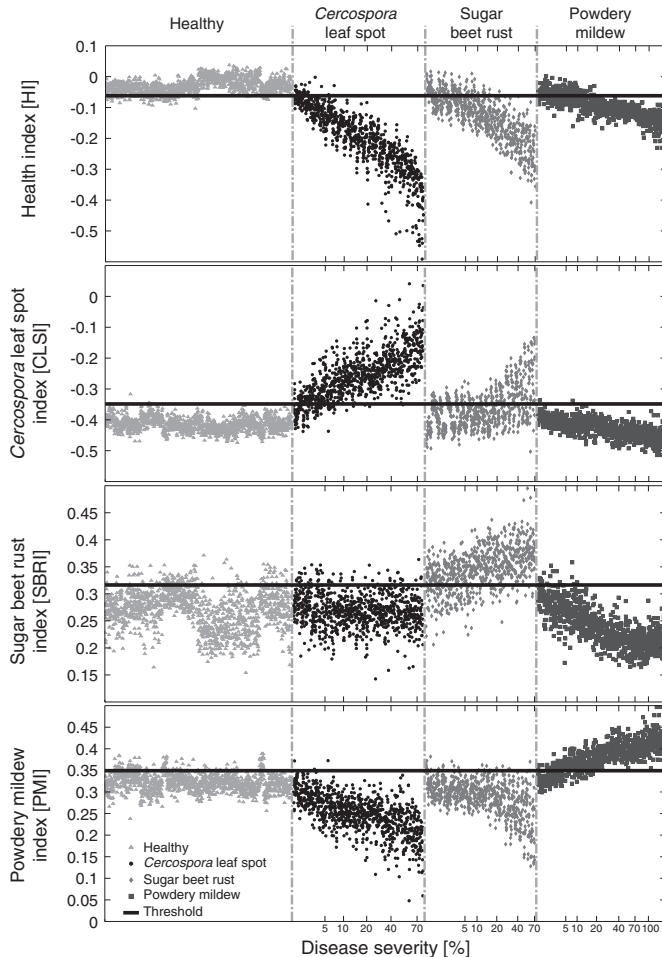


Fig. 4. Classification result based on the health-index (HI) for all disease severities over 21 days after inoculation using an 8-fold cross validation, and scatter plot of the classification based on the (A) Cercospora leaf spot-index (CLSI), (B) sugar beet rust-index (SBRI), and (C) powdery mildew-index (PMI) for all disease severities (samples ordered according to the day after inoculation).

Table 1

Classification result for each disease, based on the disease indices (DI) *Cercospora* leaf spot-index (CLSI) for the classification of *Cercospora* leaf spot, sugar beet rust-index (SBRI) for sugar beet rust detection and the powdery mildew-index (PMI) for powdery mildew detection on sugar beet leaves.

Prediction	Ground truth		Class precision
HI	All other	Healthy	
All other	129	9	93.5%
Healthy	25	148	85.6%
Class recall	83.8%	94.3%	89.0%
CLSI	All other	<i>Cercospora</i>	
All other	209	7	96.8%
<i>Cercospora</i>	8	54	87.1%
Class recall	96.3%	88.5%	92.4%
SBRI	All other	Sugar beet rust	
All other	372	15	96.1%
Sugar beet rust	25	61	70.9%
Class recall	93.7%	80.3%	87.0%
PMI	All other	Powdery mildew	
All other	363	16	95.8%
Powdery mildew	18	45	71.4%
Class recall	95.3%	73.8%	84.5%

severity. At a disease severity from 1 to 2% classification error was relatively high (51.3%) and decreased constantly to 0% at a disease severity above 16%.

The classification result based on the CLSI revealed a good separation of all classes (Fig. 4B); however, the separation of highly diseased leaves was challenging during the measuring period. Sugar beet leaves diseased with *Cercospora* leaf spot were detected with a class precision of 92.4% (Table 1). At disease severities of 1 to 2% the classification was complex (classification error of 60.1%), while all other classes were classified with a classification error of 14.1% (Table 1). The classification accuracy for *Cercospora* leaf spot diseased leaves increased with increasing disease severity. For disease severities from 6 to 9% the classification error was only 5.6% for the class *Cercospora* leaf spot, and 5% for all other classes.

Classification based on the SBRI resulted in a separation of the classes sugar beet rust to healthy, *Cercospora* leaf spot and powdery mildew (Fig. 4B). Difficulties remained in the separation of early stages of sugar beet rust infection to the other leaves. With an overall class precision of 87% the classification result was satisfying (Table 1). At low disease severities from 1 to 2% the classification error amounted 52.1% (Table 1). With increasing disease severity the classification error declined, and reached 5.8% for 25 to 30% disease severity.

Classification of the four classes by the PMI resulted in a very good separation of powdery mildew from healthy sugar beet leaves as well

Table 2

Classification error of spectral disease indices (SDIs) at different disease severity levels for each plant disease and the disease specific indices CLSI, SBRI, and PMI, respectively.

Disease severity	Classification error [%]		Classification error [%]		Classification error [%]	
	CLSI		SBRI		PMI	
	All other	CLS	All other	SBR	All other	PM
1–2 [%]	14.1	60.8	11.9	52.1	5.1	97.0
3–5 [%]	8.4	23.3	4.9	42.5	2.3	57.8
6–9 [%]	5.0	5.6	5.8	16.1	0	30.6
10–15 [%]	10.8	3.1	1.7	21.1	2.1	33.9
16–20 [%]	22.0	3.1	1.5	15.5	0.8	12.3
25–30 [%]	27.0	0	2.0	5.8	2.0	0
35–40 [%]	40.6	0	3.9	9.8	0	0
45–50 [%]	29.1	2.5	5.3	5.8	0	0
> 50 [%]	8.5	0	1.2	5.6	0.7	1.6

as from *Cercospora* leaf spot and sugar beet rust diseased sugar beet leaves with an optimized threshold value (Fig. 4). An overall class precision of 84.5% was achieved (Table 1). Difficulties remained at lower powdery mildew disease severities at disease severities of up to 9% (Table 1). Whereas all other classes were definitely detected as non-powdery mildew diseased by this index (classification error: 0% to 5.1%), the classification error for powdery mildew identification was high (classification error: 97.0% to 1.6%). At disease severity above 25%, a perfect classification (classification error 0%) was obtained (Table 2).

3.3. Comparison with common vegetation indices

The new developed SDIs had higher classification accuracy compared to common vegetation indices like the NDVI or pigment specific indices (Table 3). The classification accuracy of the HI was best (89.0%) for the differentiation of healthy and diseased sugar beet leaves, followed by ZM, PRI, PSSRb and ARI with classification accuracies of 85.4%, 83.5%, 83.1%, and 82.7%, respectively (Table 3). Classification of *Cercospora* leaf spot diseased leaves was best using CLSI with a classification accuracy of 92.4%. The mCAI, ARI, and PRI showed acceptable classification accuracies (89.5%, 84.8%, and 82.6%, respectively). However the recall clarified, that all vegetation indices had low classification accuracies for the identification of *Cercospora* diseased leaves, and high accuracies only for the detection of all other leaves (Table 3). In general SVIs are unsuitable to detect sugar beet rust and powdery mildew; the classification accuracy was 50% for all applied SVIs.

Table 3

Comparison of the classification ability of the health-index (HI) and the *Cercospora* leaf spot index (CLSI) and common spectral vegetation indices (SVIs): NDVI normalized difference vegetation index, PRI Photochemical reflectance index, ARI anthocyanin reflectance index, mCAI modified chlorophyll absorption integral, PSSRa pigment specific simple ratio chlorophyll a, PSSRb pigment specific simple ratio chlorophyll b, and PSSRc pigment specific simple ratio carotenoids.

Index	Classification accuracy	Recall	
		Healthy	All other
HI	89.0%	94.3%	83.8%
NDVI	80.3%	89.9%	70.8%
PRI	83.5%	88.5%	78.5%
ARI	82.7%	86.7%	78.6%
SICI	74.5%	86.8%	62.3%
mCAI	77.0%	92.4%	61.5%
PSSRa	78.8%	78.7%	78.9%
PSSRb	83.1%	79.4%	86.7%
PSSRc	57.3%	18.8%	95.9%
GM1	82.7%	77.2%	88.2%
GM2	82.4%	71.5%	93.3%
ZM	85.4%	78.6%	92.2%
TCARI/OSAVI	77.5%	64.2%	90.8%
Index	Classification accuracy	Recall	
		<i>Cercospora</i>	All other
CLSI	92.4%	88.5%	96.3%
NDVI	73.4%	48.4%	98.3%
PRI	82.6%	68.1%	97.2%
ARI	84.8%	70.0%	99.7%
SICI	74.7%	55.6%	93.9%
mCAI	89.5%	79.7%	99.3%
PSSRa	69.6%	42.1%	97.0%
PSSRb	69.6%	41.1%	98.1%
PSSRc	50.0%	0.0%	100.0%
GM1	50.0%	0.0%	100.0%
GM2	69.5%	41.2%	97.7%
ZM	66.6%	35.7%	97.4%
TCARI/OSAVI	50.7%	1.4%	1.0%

3.4. Application of spectral disease indices on independent data sets

An implementation of the developed SDIs was proven on two different independent data sets. Due to different light conditions and sensor specification it was necessary to calculate the thresholds for disease classification individually for each dataset. In the field experiment powdery mildew and *Cercospora* leaf spot were the predominant diseases during vegetation period (see Mahlein et al. (2009) for details). In most cases both diseases occurred as mixed infections of sugar beet plants. A classification of non-imaging spectroradiometer data from the canopy scale based on the HI was possible with an accuracy of 81.63% (Fig. 5). Due to the high incidence of mixed infection a classification based on a disease specific index was not suitable.

The different SDIs were calculated pixel wise on hyperspectral imaging data of a *Cercospora* leaf spot diseased leaves under controlled conditions (Fig. 6). The HI was suitable to detect all symptomatic necrotic lesions on the sugar beet leaf with an accuracy of 95.91% and all characteristic symptoms were detected as non-healthy. In a next step the disease specific indices were applied on the imaging data. A specific classification of *Cercospora* leaf spots was possible with an accuracy of 95.9% using the CLSI, whereas the PMI and the SBRI were not sensitive to *Cercospora* leaf spot symptoms. Detailed information on the classification result can be found in the supplementary data, Appendix C.

4. Discussion

As shown in previous work, foliar diseases of sugar beet impact the spectral signature of sugar beet leaves in different ways, depending on the biology of the pathogens and the characteristic host-pathogen interaction (Mahlein et al., 2010; Mahlein et al., 2012b; Rumpf et al., 2010). The present study provides evidence that spectral disease indices (SDIs) will improve and simplify plant disease detection based on hyperspectral data. The developed SDIs are based on the most relevant wavelength and normalized wavelength combinations regarding to a plant disease. They are characterized by a high sensitivity and specificity for the detection and identification of the different foliar diseases of sugar beet.

According to Blackburn (2007) recent research for optimizing SVIs resulted in the incorporation of more than two narrow wavebands from the visible region, the red edge or the near infrared. Depending on the measuring scale three band indices (leaf-scale) or four band

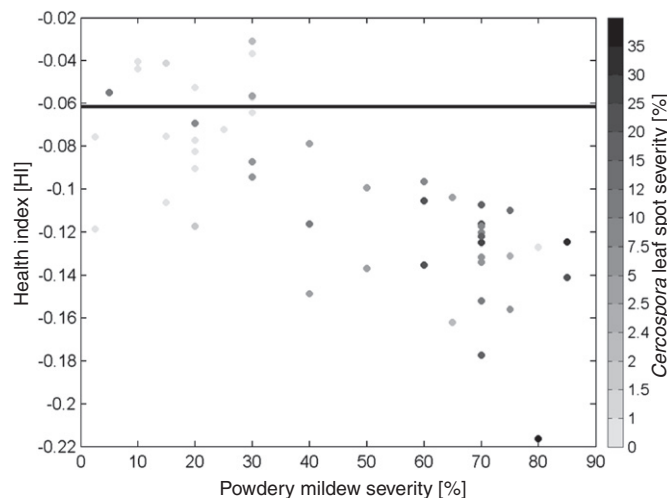


Fig. 5. Classification result based on the application of the health-index (HI) on spectroradiometer data from a field experiment on the canopy scale. Areas of the sugar beet field diseased with powdery mildew and *Cercospora* leaf spot were classified correctly with an accuracy of 81.63%. The gray scale represents disease severity of *Cercospora* leaf spot.

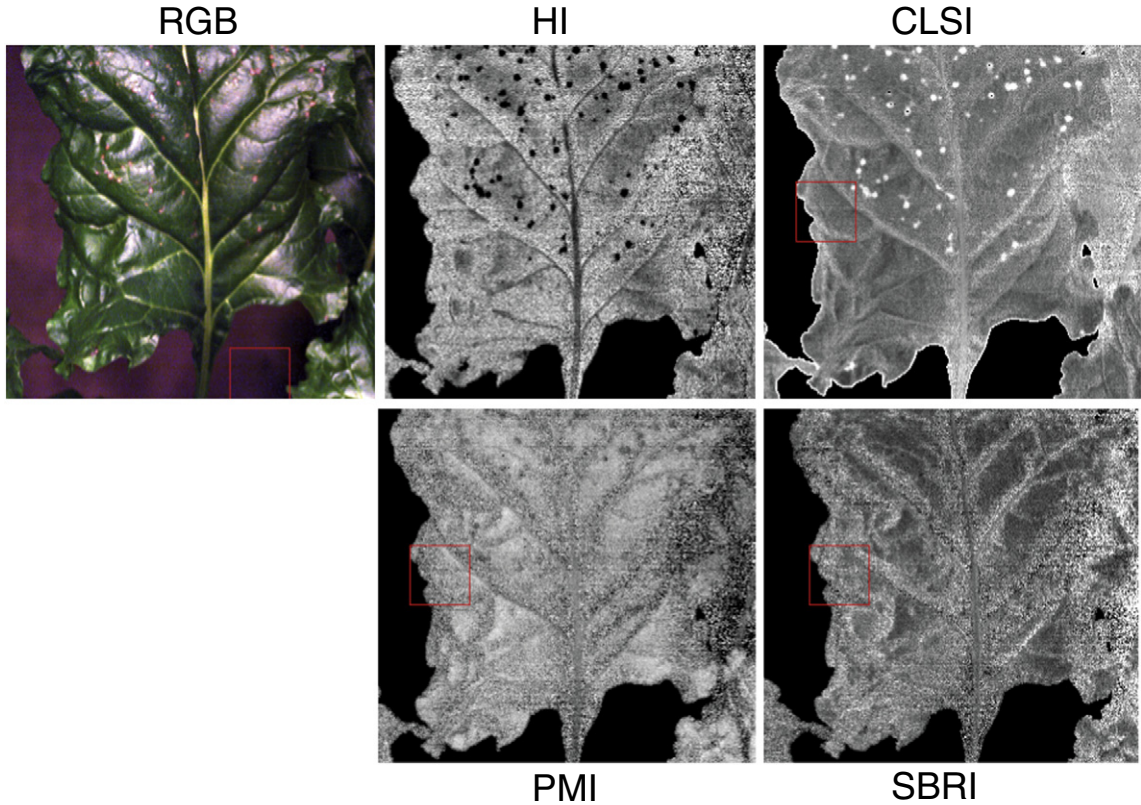


Fig. 6. RGB-image from a hyperspectral image of a *Cercospora* leaf spot diseased sugar beet leaf and gray-scale pixel-wise classification using the developed spectral disease indices (SDIs). Light-colored pixels indicate high index values and dark pixels vice versa. (HI: health-index, CLSI: *Cercospora* leaf spot-index, SBRI: sugar beet rust-index, PMI: powdery mildew-index).

indices (canopy-scale) are generally applicable (Gitelson et al., 2003; Sims & Gamon, 2002; Thenkabail et al., 2000).

The common way to detect significant wavelength for SVI development is by correlation to a biochemical or biophysical trait (Gitelson & Merzlyak, 1996; Hatfield et al., 2008). For the development of qualitative SDIs the RELIEF-F algorithm offers multiple advantages. Since RELIEF-F is dealing with non-linear classes, a separation of the different classes becomes possible by aggregating all other data in one class. The correlation coefficient would be improper in this case. To reduce the impact of different illumination, topography, crop variety or sensor specific effects, the wavelength differences of all SDIs were normalized (Jackson, 1986; Lillesand & Kiefer, 2000; Lyon et al., 1998). By applying this concept, an improved robustness and generalization ability of the developed SDIs to independent data sets were reached. Moreover, the generalization ability of the developed indices was improved by cross validation by taking the entire data set into account. In this way variances between different experiments under similar conditions have been considered.

With the health-index a first binary classification into healthy and diseased sugar beet plants was possible. In a next step spectral disease indices were developed for an identification of each disease. The indices HI, CLSI and SBRI are based on reflectance at narrow bands centered around 700 nm. As Gitelson and Merzlyak (1996) pointed out, reflectance near 700 nm is a fundamental feature of green vegetation produced by an equilibrium between biochemical and biophysical plant characteristics. The blue shift of the reflectance curve red edge frequently accompanies stress, and could provide early detection of plant stress for most causes of stress (Carter & Miller, 1994; Gitelson & Merzlyak, 1994). Since plant diseases influence the chlorophyll content of crop plants, increased reflectance around 700 nm can be a first but unspecific indicator to detect diseased crops.

Foliar pathogens affect photosynthetic activity of infected leaves by reducing the green leaf area; an effect on photosynthesis in

asymptomatic areas is reported as well (Robert et al., 2005). Interestingly, reflectance next to 700 nm is combined in HI with reflectance at 534 nm. According to Gamon et al. (1992) reflectance at 531 nm can detect the interconversion of the xanthophyll cycle pigments. Since xanthophyll cycle pigments are regulatory pigments linked to PSII light use efficiency, reflectance indices incorporating reflectance next to 531 nm could provide an indicator of photosynthetic function (Gamon et al., 1992; Rascher et al., 2010). The identification of diseases was a more complex problem, since different diseases may influence crop plants in a similar way. The main influence of *Cercospora* leaf spot to leaf reflectance was in the VIS from 550 to 700 nm and in the NIR from 700 nm to 850 nm, respectively. These regions are influenced by the chlorophyll and brown pigment content as well as by the water content and structural changes (Peñuelas & Filella, 1998). As a perthotroph pathogen *C. beticola* causes necrotic, coalescing leaf spots due to membrane damage and cell death after the fungus has penetrated the leaf stomata (Daub & Ehrenshaft, 2000). In consequence, the chlorophyll content decreases and leaf tissue structure is impaired. Reflectance in the NIR is mainly influenced by leaf tissue structure, in detail by internal scattering processes due to air spaces, water content and air–water interfaces (Asner, 1998; Ustin & Gamon, 2010; Ustin et al., 2009). Therefore, normalized reflectance difference with 698 nm and 570 nm and constant reflectance at 734 nm was a reliable indicator for *Cercospora* leaf spot infestation.

The SBRI, using three narrow bands in the visible and red edge (i.e. 513 nm, 570 nm and 704 nm) offered a robust solution for the detection of sugar beet rust. According to Merzlyak et al. (1999) reflectance from 510 nm to 520 nm represents the absorption maximum of carotenoids. It is well documented that urediniospores of rust fungi contain a high concentration of carotenoids and melanin-like pigments, causing the characteristic brown-orange color (Hougen et al., 1959; Trocha et al., 1974). Furthermore reflectance at 513 nm, before the

green peak, and 570 nm, behind the green peak, is mainly influenced by the chlorophyll content and can be used as an indicator for the chlorophyll/carotenoid ratio (Blackburn, 1998a; Blackburn, 1998b; Richardson et al., 2002). Reflectance at 704 nm as single wavelength is next to the red-edge inflection point (Carter & Miller, 1994; Gitelson & Merzlyak, 1994). Nevertheless, the small size of rust colonies impeded the detection in early stages or at low disease severities.

Similarly, an unambiguous detection of powdery mildew in early stages is challenging. First symptoms are fluffy white mycelia covering the leaf surface which affects the external reflectance and spectral signature like a dusty coat. The overall reflectance increase with increasing powdery mildew disease severity was the contributing factor in case of the PMI (Mahlein et al., 2010). By using normalized reflectance differences this difficulty has been taken into consideration. Powdery mildew was the only pathogen, causing changes in leaf reflectance in the blue region, and throughout the NIR. This effect, caused by the white powdery mycelium covering the leaf surface is similar to increasing the light intensity. Jackson and Huete (1991) described that ratios are sensitive to increasing solar intensity, which was successfully adopted for the development of PMI by using normalized differences.

For specific classification of plant diseases comparative studies have demonstrated that SDIs are superior to common SVIs. A successful application to independent data sets from the canopy scale and from a hyperspectral imaging sensor is encouraging for precision crop protection applications in the near future. It should be stressed, however, that the applicability of SDIs to datasets, assessed under changing conditions includes several difficulties. Particularly the threshold value has to be optimized prior to classification. Notwithstanding it can be affirmed, that the proposed method to develop SDIs can be transferred to hyperspectral data from different kinds of sensors, from various scales, and for different kinds of biotic and abiotic stress of crops.

5. Conclusion

All four developed spectral disease indices (SDIs) resulted in a high specificity and sensitivity for detecting and identifying plant diseases. Difficulties still remained at early infection stages, due to minor changes in leaf reflectance. For the first time SDIs, developed on disease significant single wavelength and normalized wavelength differences have been applied for non-invasive detection of crop diseases. Using these SDI diseases can be identified and differentiated, which is not possible when using vegetation indices sensitive to abiotic stress conditions, e.g. indices related to chlorophyll content. A first feasibility study demonstrated that SDIs can be used on independent data sets from different kinds of sensors and different measuring setups. Nevertheless we expect, that the use of hyperspectral imaging data for the development of SDIs will further improve the sensitivity and specificity of disease detection in near future. SDIs are of high interest for precision crop protection via reduction of data dimensionality and computationally efficient data analysis and processing. Additionally, the statistical approach for the development of SDIs can be transferred and generalized for other plant pathogen systems. Based on the *a priori* knowledge on required band settings a simple and cheap sensor that only measures reflectance at narrow bands centered at significant wavelength can be configured. This radiometer could instantaneously calculate SDIs, and, by using appropriate calibration functions, give the estimation of disease severity in seconds. Further work will be needed to transfer the developed SDIs into praxis and to test the applicability for a precise, reproducible and time saving disease monitoring on the canopy and field scale with different sensors.

Acknowledgments

This study has been conducted within the Research Training Group 722 'Information Techniques for Precision Crop Protection', funded by

the German Research Foundation (DFG). The authors would like to thank the editor and reviewers for their valuable comments and suggestions to improve the quality of this paper.

Appendix A. Supplementary data

Supplementary data to this article can be found online at <http://dx.doi.org/10.1016/j.rse.2012.09.019>.

References

- Asner, G. (1998). Biophysical and biochemical sources of variability in canopy reflectance. *Remote Sensing of Environment*, 64, 234–253.
- Blackburn, G. A. (1998a). Quantifying chlorophylls and carotenoids at leaf and canopy scale: an evaluation of some hyperspectral approaches. *Remote Sensing of Environment*, 66, 273–285.
- Blackburn, G. A. (1998b). Spectral indices for estimating photosynthetic pigment concentrations: a test using senescent tree leaves. *International Journal of Remote Sensing*, 19(4), 657–675.
- Blackburn, G. A. (2007). Hyperspectral remote sensing of plant pigments. *Journal of Experimental Botany*, 58, 844–867.
- Blackburn, G. A., & Steele, C. M. (1999). Towards the remote sensing of matorral vegetation physiology: Relationships between spectral reflectance, pigment, and biophysical characteristics of semiarid bushland canopies. *Remote Sensing of Environment*, 70, 278–292.
- Carter, G. A., & Miller, R. L. (1994). Early detection of plant stress by digital imaging with narrow stress-sensitive wavebands. *Remote Sensing of Environment*, 50, 295–302.
- Daub, M. E., & Ehrenshaft, M. (2000). The photoactivated *Cercospora* toxin cercosporin: Contributions to plant disease and fundamental biology. *Annual Review of Phytopathology*, 38, 461–490.
- Delalieux, S., Somers, B., Verstraeten, W. W., van Aardt, A. N. J., Keulemans, W., & Coppin, P. (2009). Hyperspectral indices to diagnose leaf biotic stress of apple plants, considering leaf phenology. *International Journal of Remote Sensing*, 30(8), 1887–1912.
- Doraiswamy, P. C., Moulin, S., Cook, P. W., & Stern, A. (2003). Crop yield assessment for remote sensing. *Photogrammetric Engineering and Remote Sensing*, 69, 665–674.
- Galvao, L. S., Roberts, D. A., Formaggio, A. R., Numata, I., & Breunig, F. M. (2009). View angle effects on the discrimination of soybean varieties and on the relationships between vegetation indices and yield using off-nadir hyperion data. *Remote Sensing of Environment*, 113, 846–856.
- Gamon, J. A., Peñuelas, J., & Field, C. B. (1992). A narrow-waveband spectral index that tracks diurnal changes in photosynthetic efficiency. *Remote Sensing of Environment*, 41, 35–44.
- Gitelson, A. A., Gritz, Y., & Merzlyak, M. N. (2003). Relationships between leaf chlorophyll content and spectral reflectance and algorithms for non-destructive chlorophyll assessment in higher plant leaves. *Journal of Plant Physiology*, 160, 271–282.
- Gitelson, A. A., Kaufman, Y. J., Stark, R., & Rundquist, D. (2002). Novel algorithms for remote estimation of vegetation fraction. *Remote Sensing of Environment*, 80, 76–87.
- Gitelson, A. A., & Merzlyak, M. N. (1994). Spectral reflectance changes associate with autumn senescence of *Aesculus hippocastanum* L. and *Acer platanoides* L. leaves. Spectral features and relation to chlorophyll estimation. *Journal of Plant Physiology*, 143, 286–292.
- Gitelson, A. A., & Merzlyak, M. N. (1996). Remote estimation of chlorophyll content in higher plant leaves. *Journal of Plant Physiology*, 148, 494–500.
- Gitelson, A. A., & Merzlyak, M. N. (1997). Signature analysis of leaf reflectance spectra: Algorithm development for remote sensing of chlorophyll. *International Journal of Remote Sensing*, 18, 2691–2697.
- Gitelson, A. A., Merzlyak, M. N., & Chivkunova, B. O. (2001). Optical properties and non-destructive estimation of anthocyanin content in plant leaves. *Photochemistry and Photobiology*, 74, 38–45.
- Haboudane, D., Miller, J. R., Tremblay, N., Zarco-tejada, P. J., & Dextraze, L. (2002). Integrated narrow-band vegetation indices for prediction of crop chlorophyll content for application to precision agriculture. *Remote Sensing of Environment*, 81, 416–426.
- Hatfield, L. J., Gitelson, A. A., Schepers, S. J., & Walther, L. C. (2008). Application of spectral remote sensing for agronomic decisions. *Agronomy Journal*, 100(3), 117–131.
- Hillnhütter, C., & Mahlein, A.-K. (2008). Early detection and localisation of sugar beet diseases: New approaches. *Gesunde Pflanzen*, 60(4), 143–149.
- Hillnhütter, C., Mahlein, A.-K., Sikora, R., & Oerke, E.-C. (2011). Remote sensing to detect plant stress induced by heterodera schachtii and rhizoctonia solani in sugar beet fields. *Field Crops Research*, 122(1), 70–77.
- Hougen, F., Craig, B., & Ledingham, D. (1959). The oil of wheat stem rust uredospores. I. the sterol and carotenes of the unsaponifiable matter. *Canadian Journal of Microbiology*, 4, 521–529.
- Jackson, R. D. (1986). Remote sensing of biotic and abiotic plant stress. *Annual Review of Phytopathology*, 24, 265–287.
- Jackson, R. D., & Huete, A. R. (1991). Interpreting vegetation indices. *Preventive Veterinary Medicine*, 11, 185–200.
- Jacquemoud, S., & Baret, F. (1990). Prospect: a model of leaf optical properties spectra. *Remote Sensing of Environment*, 34, 75–91.
- Kononenko, I. (1994). Estimating attributes: Analysis and extensions of relief. *Proceedings of the European conference on machine learning on machine learning* (pp. 171–182). Secaucus, NJ, USA: Springer-Verlag New York, Inc.

- Laudien, R., Bareth, G., & Doluschitz, R. (2003). Analysis of hyperspectral field data for detection of sugar beet diseases. *Proceedings of the EFITA Conference, Debrecen, Hungary* (pp. 375–381).
- Lillesand, T. M., & Kiefer, R. W. (2000). *Remote sensing and image interpretation*. New York, NY, USA: John Wiley & Sons, Inc.
- Lyon, J., Yuan, D., Lunetta, R., & Elvidge, C. (1998). A change detection experiment using vegetation indices. *Photogrammetric Engineering and Remote Sensing*, 64(2), 143–150.
- Mahlein, A. -K., Hillnhütter, C., Mewes, T., Scholz, C., Steiner, U., Dehne, H. -W., et al. (2009). Disease detection in sugar beet fields: A multi-temporal and multi-sensor approach on different scales. In C. M. Neale, & A. Maltese (Eds.), *Proceedings of the SPIE Europe Conference on Remote Sensing, Vol. 7472*, (747228–747238–10).
- Mahlein, A. -K., Oerke, E. -C., Steiner, U., & Dehne, H. -W. (2012). Recent advances in sensing plant diseases for precision crop protection. *European Journal of Plant Pathology*, 133(1), 197–209.
- Mahlein, A. -K., Steiner, U., Dehne, H. -W., & Oerke, E. -C. (2010). Spectral signatures of sugar beet leaves for the detection and differentiation of diseases. *Precision Agriculture*, 11(4), 413–431.
- Mahlein, A. -K., Steiner, U., Hillnhütter, C., Dehne, H. -W., & Oerke, E. -C. (2012). Hyperspectral imaging for small-scale analysis of symptoms caused by different sugar beet diseases. *Plant methods*, 8(1), 3.
- Merzlyak, M. N., Gitelson, A. A., Chivkunova, O. B., & Rakitin, V. Y. (1999). Non-destructive optical detection of pigment changes during leaf senescence and fruit ripening. *Physiologia Plantarum*, 106, 135–141.
- Moshou, D., Bravo, C., West, J., Wahlen, S., McCartney, A., & Ramon, H. (2004). Automatic detection of 'yellow rust' in wheat using reflectance measurements and neural networks. *Computers and Electronics in Agriculture*, 44, 173–188.
- Nutter, F. W. J., Littrell, R. H., & Brennemann, T. B. (1990). Utilization of a multispectral radiometer to evaluate fungicide efficacy to control late leaf spot in peanut. *Phytopathology*, 80, 102–108.
- Oerke, E. -C., Steiner, U., Dehne, H. -W., & Lindenthal, M. (2006). Thermal imaging of cucumber leaves affected by downy mildew and environmental conditions. *Journal of Experimental Botany*, 57, 2121–2132.
- Peñuelas, J., Baret, F., & Filella, I. (1995). Semiempirical indices to assess carotenoids/chlorophyll a ratio from leaf spectral reflectance. *Photosynthetica*, 31, 221–230.
- Peñuelas, J., & Filella, I. (1998). Visible and near-infrared reflectance techniques for diagnosing plant physiological status. *Trends in Plant Science*, 3, 151–156.
- Peñuelas, J., Filella, I., Biel, C., Serrano, L., & Save, R. (1993). The reflectance at the 950–970 nm region as an indicator of plant water status. *International Journal of Remote Sensing*, 14(10), 1887–1905.
- Rascher, U., Damm, A., van der Linden, S., Okujeni, A., Pieruschka, R., Schickling, A., et al. (2010). Sensing of photosynthetic activity of crops. In E. -C. Oerke, R. Gerhards, G. Menz, & R. A. Sikora (Eds.), *Precision crop protection – The challenge and use of heterogeneity* (pp. 87–100). Dordrecht, Netherlands: Springer.
- Richardson, A., Duigan, S., & Berlyn, G. (2002). An evaluation of noninvasive methods to estimate foliar chlorophyll content. *The New Phytologist*, 153(1), 185–194.
- Robert, C., Bancal, M., Ney, B., & Lannou, C. (2005). Wheat leaf photosynthesis loss due to leaf rust, with respect to lesion development and leaf nitrogen status. *The New Phytologist*, 165(1), 227–241.
- Robnik-Šikonja, M., & Kononenko, I. (2003). Theoretical and empirical analysis of relief and rrelief. *Machine Learning*, 53(1), 23–69.
- Rouse, J. W., Haas, R. H., Schell, J. A., & Deering, D. W. (1974). Monitoring vegetation systems in the Great Plains with ERTS. *Proc. 3rd Earth Resources Technology Satellite-1 Symposium, Greenbelt, MD NASA* (pp. 301–317).
- Rumpf, T., Mahlein, A. -K., Steiner, U., Oerke, E. -C., Dehne, H. -W., & Plümer, L. (2010). Early detection and classification of plant diseases with support vector machines based on hyperspectral reflectance. *Computers and Electronics in Agriculture*, 74, 91–99.
- Sims, D., & Gamon, J. (2002). Relationships between leaf pigment content and spectral reflectance across a wide range of species, leaf structures and developmental stages. *Remote Sensing of Environment*, 81(2), 337–354.
- Steddom, K., Bredehoeft, W. M., Khan, M., & Rush, M. C. (2005). Comparison of visual and multispectral radiometric disease evaluations of *Cercospora* leaf spot of sugar beet. *Plant Disease*, 89(2), 153–158.
- Steiner, U., Bürling, K., & Oerke, E. -C. (2008). Sensor use in plant protection. *Gesunde Pflanzen*, 60(4), 131–141.
- Thenkabail, P. S., Smith, R. B., & De Pauw, E. (2000). Hyperspectral vegetation indices and their relationship with agricultural crop characteristics. *Remote Sensing of Environment*, 71, 158–182.
- Trocha, P., Daly, J., & Langenbach, R. (1974). Cell walls of germinating uredospores: I. Amino acid and carbohydrate constituents 1. *Plant Physiology*, 53, 519.
- Ustin, S. L., & Gamon, J. A. (2010). Remote sensing of plant functional types. *The New Phytologist*, 186, 795–816.
- Ustin, S. L., Gitelson, A. A., Jaquemoud, S., Schaepman, M., Asner, G. P., Gamon, J. A., et al. (2009). Retrieval of foliar information about plant pigment systems from high resolution spectroscopy. *Remote Sensing of Environment*, 113, 67–77.
- Wolf, P. F. J., & Verreet, A. J. (2002). The IPM sugar beet model, an integrated pest management system in Germany for the control of fungal leaf diseases in sugar beet. *Plant Disease*, 86(4), 336–344.
- Zarco-Tejada, P. J., Miller, J. R., Mohammed, G. H., Notland, T. L. L., & Sampson, P. H. (2001). Scaling-up and model inversion methods with narrow-band optical indices for chlorophyll content estimation in closed forest canopies with hyperspectral data. *IEEE Transactions on Geoscience and Remote Sensing*, 39, 1491–1507.